

Compact spectral shearing interferometer for ultrashort pulse characterization

Aleksander S. Radunsky

Institute of Optics, University of Rochester, Rochester, New York 14627, USA, and Clarendon Laboratory, University of Oxford, Parks Road, Oxford OX1 3PU, UK

Ian A. Walmsley, Simon-Pierre Gorza, and Piotr Wasylczyk

Clarendon Laboratory, University of Oxford, Parks Road, Oxford OX1 3PU, UK

Received July 21, 2006; revised October 7, 2006; accepted October 11, 2006;
posted October 18, 2006 (Doc. ID 73299); published December 23, 2006

A simple, compact, and robust implementation of spectral shearing interferometry using a single nonlinear crystal for both ancilla generation and upconversion is demonstrated. The device is capable of accurate characterization of femtosecond laser pulses over the 740–900 nm range with a KDP crystal. © 2006 Optical Society of America

OCIS codes: 320.7160, 320.7100, 190.4360.

The widespread use of ultrafast technology in physics, chemistry, biology, and medicine and its enabling role in numerous practical applications call for the development of pulse characterization instrumentation that is at least as robust as the current generation of laser sources.^{1–4} Spectral phase interferometry for direct electric-field reconstruction⁵ (SPIDER) is a well-known accurate, precise, reliable, and rapid self-referencing interferometric technique for characterizing ultrashort pulses. Recording of the spectral interferogram generated by a pair of spectrally shifted replicas of the measured pulse is followed by a noniterative algorithm to retrieve the pulse spectral amplitude and phase. Recently we showed that a thick nonlinear crystal with an appropriately tailored phase-matching function (PMF) may be used to generate the spectral shear, eliminating the requirement for linearly chirped ancillary pulses and the optical components to produce them.⁶

In this Letter we introduce a streamlined, robust, and compact spectral shearing interferometry (SSI) implementation and demonstrate its performance for a range of pulses of different bandwidths and center wavelengths that is much wider than would be expected from the simple application of the tailored PMF concept. In keeping with established practice in the field, we name it ARAIGNEE (Another Ridiculous Acronym for Interferometric Geometrically simplified Noniterative *E*-field Extraction).

In a sufficiently long nonlinear crystal oriented for type II sum-frequency generation (SFG) the incident pulse propagating as an ordinary wave (*o*-wave) has a large acceptance bandwidth, whereas the extraordinary wave (*e*-wave) has a much narrower acceptance bandwidth. This highly asymmetric PMF shape is due to a group-velocity (GV) match between the *o*-fundamental input and the *e*-upconverted output and a GV mismatch between the *e*-fundamental and the *e*-upconverted fields.⁷ As a result, the ordinary test pulse is upconverted with a single *e*-ray frequency, resulting in its replication at the upconverted frequency. The angle of propagation relative to the crystal optic axis determines the frequency of the

narrowband component of the *e*-wave, which upconverts with the entire spectrum of the *o*-wave, enabling the spectral shear necessary for SSI. However, this simple argument does not provide enough details to enable the full range of operation to be derived, and we have therefore developed a more comprehensive wave mixing model.

Figure 1 displays the schematic of a compact ARAIGNEE setup. The horizontally polarized test pulse passes through a zero-order $\lambda/2$ wave plate (optic axis at 22.5° with respect to horizontal) and a quartz plate (10 mm thick, slow axis horizontal); these two elements separate the pulse into the ordinary and extraordinary polarizations, with the *e*-wave being predelayed by 317 fs with respect to the *o*-wave, enabling a distortionless upconversion in the crystal.⁸

The beam is subsequently sent onto a pair of mirrors adjacent to each other with a small offset d along the beam propagation direction, and a small mutual horizontal tilt β that splits the incident beam into two beams (see detail in Fig. 1). The two beams are directed into a KDP crystal (5 mm thick, cut for second harmonic generation at 830 nm, optic axis horizontal) where each beam undergoes type II SFG. The resulting SFG pulses are spectrally shifted (sheared) owing to the angular offset (2β) of the fundamental beams in the crystal. In our experiment, the angle β

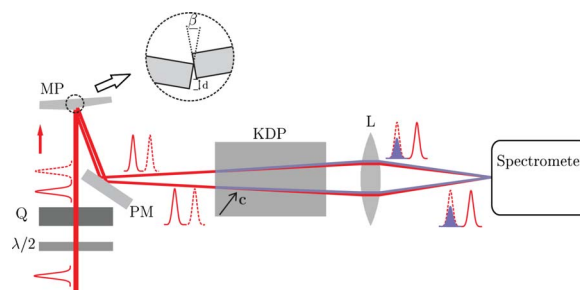


Fig. 1. (Color online) Schematic of the ARAIGNEE device. $\lambda/2$, half-wave plate; Q, quartz plate; MP, mutually tilted (by β) and longitudinally shifted (by d) mirror pair; PM, pick-off mirror; KDP, nonlinear crystal; L, lens. Dotted curves, ordinary pulses; solid curves, extraordinary pulses.

has been set to 0.25° , resulting in a spectral shear of about 0.8 nm. No great accuracy is necessary in setting the angle β , because the actual value of the spectral shear is easily measured from the two individually recorded SFG spectra. The delay between the SFG pulses (≈ 1.5 ps), required for recording the SPIDER interferogram, is achieved by setting the offset d to ≈ 225 μm . At the output of the crystal, the two beams are overlapped with a 10 cm lens onto the entrance slit of a compact grating spectrometer (USB2000, Ocean Optics). The entire arrangement easily fits onto a 20×20 cm breadboard, is easy to align, and produces a standard SPIDER interferogram. The delay calibration is performed with the simultaneously recorded interferogram from the two pairs of extraordinary red and blue pulses.⁹

Two laser sources were used to evaluate the performance of ARAIGNEE: a tunable MaiTai (Spectra-Physics), delivering ≈ 70 fs (intensity FWHM: $\Delta\omega \approx 35$ mrad fs⁻¹) pulses centered in the 750–850 nm range, and a Mira Seed (Coherent), providing broader bandwidth ($\Delta\omega \approx 80$ mrad fs⁻¹) pulses. The input beam waists at the mirror pair were ≈ 3 –5 mm (no beam expansion or focusing was necessary). With ARAIGNEE's refresh rate of a few hertz, the average input power could be attenuated to ≈ 1 mW before the signal reached the noise level. The results of the spectral phase reconstruction for pulses of different bandwidth and center frequency are shown in Fig. 2. The solid curve plots show the retrieved spectral phase added to three distinct test pulses after propagation through different blocks of the BK7 glass, indicating a very good agreement between the retrieved and calculated (from the Sellmeier coefficients) data. The input pulse spectral phases were independently verified with a conventional SPIDER apparatus. The measurements in Fig. 2 were taken over a considerably broader tuning range than would be expected from the simple interpretation of the tailored PMF concept.⁶

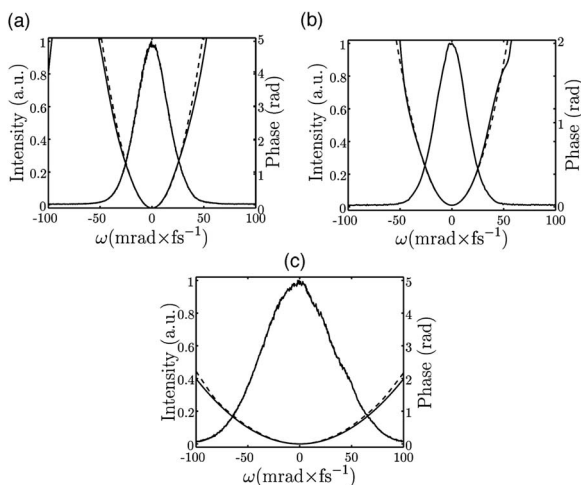


Fig. 2. Measured (solid curves) and calculated (dashed curves) spectral phase and measured spectral intensity for different central wavelengths and bandwidths of the input pulse (a) $\lambda_c = 830$ nm, $\Delta\omega = 35$ mrad fs⁻¹, 100 mm BK7 glass block; (b) $\lambda_c = 760$ nm, $\Delta\omega = 35$ mrad fs⁻¹, 28.5 mm BK7; (c) $\lambda_c = 830$ nm, $\Delta\omega = 80$ mrad fs⁻¹, 9.5 mm BK7.

Consider a type II SFG interaction leading to generation of the two frequency-sheared replicas. For each replica there are three interacting pulses in the process: the input *o*-wave, the input *e*-wave, and the extraordinary polarized upconverted output (SF *e*-wave). Let $A_o(t)$, $A_e(t)$, and $A_{\text{SF}}(t)$ be the slowly varying complex amplitude envelopes of these pulses. Assuming that the amplitude envelopes of the two fundamental pulses do not change during propagation in the nonlinear crystal, the SF-wave in the nonlinear crystal obeys the equation

$$\frac{\partial}{\partial z} A_{\text{SF}}(t, z) = i\Gamma A_o(t - \Delta k'_{\text{SF}o} z) A_e(t - \Delta k'_{\text{SF}e} z - t_0)^{i\Delta k z}, \quad (1)$$

where Γ characterizes the nonlinear response of the medium, t_0 is the delay between the two fundamental pulses at the crystal input, and t is the time in a reference frame traveling at the GV of the pulse at the frequency $\omega_{\text{SF}} = \omega_o + \omega_e$, where ω_j ($j = o, e$) are the carrier frequencies of the two fundamental waves. We also assume the GV match between the fundamental *o*-wave and the SF *e*-wave (i.e., $\Delta k'_{\text{SF}o} = k'_{\text{SF}} - k'_o \approx 0$; k' is the inverse of the GV) and a GV mismatch between the fundamental *e*-wave and the SF *e*-wave (i.e., $\Delta k'_{\text{SF}e} = k'_{\text{SF}} - k'_e \neq 0$). Integration of Eq. (1) over the crystal length results in the following solution for the SF-wave:

$$A_{\text{SF}}(t) \propto \exp(-i\Omega t) \bar{A}_e(\Omega) A_o(\alpha t + t_\Delta), \quad (2)$$

providing the faster pulse overtakes the slower one during propagation (and the pulses do not overlap either before or after the crystal), and $\Delta k'_{\text{SF}o} / \Delta k'_{\text{SF}e} \ll 1$, where $\alpha = (1 - \Delta k'_{\text{SF}o} / \Delta k'_{\text{SF}e})$ and $t_\Delta = -t_0 \Delta k'_{\text{SF}o} / \Delta k'_{\text{SF}e}$. Ω denotes the spectral detuning of the upconverted field from the central frequency ω_{SF} at perfect phase matching, while $\bar{A}_e(\Omega)$ is the magnitude of the spectral density of the *e*-polarized pulse at the frequency $\omega_e + \Omega$. We can thus interpret the upconversion process as a waveform transfer from the *o*-wave to the SF *e*-wave by mixing a quasi-monochromatic slice of the spectrum of the *e*-wave with the whole spectrum of the *o*-wave.¹⁰ The actual frequency of the quasi-monochromatic slice $\omega_e + \Omega$ is defined by the PMF; i.e., the shear between the two replicas, essential for SSI, is generated by adjusting the angle of propagation of the pulses in the crystal. Relation (2) also shows that for pulses in the spectral regions where $\Delta k'_{\text{SF}o} \neq 0$ the SF pulse replicates the input pulse up to a known time axis scaling factor α that depends only on the crystal dispersion.¹¹

As mentioned before, the two fundamental pulses must be predelayed so that they entirely walk through one another while propagating in the crystal. This imposes the limits on the measured pulse durations and bandwidths. For a given crystal length L , the maximum temporal support window δt of the test pulse accurately is $\delta t \approx |\Delta k'_{oe}| L / 2$, where $|k'_{oe}|$ is the GV mismatch between the *e*- and *o*-waves. This is the equivalent of the requirement for a conventional

SPIDER that the unknown pulse is mixed in the nonlinear crystal with a quasi-monochromatic slice of the stretched pulse. On the other hand, the maximum pulse bandwidth is set by the requirement that all spectral components of the *o*-fundamental pulse travel slower than the spectral components of the *e*-fundamental pulse, i.e., $\delta\omega \ll (|k'_o| - |k'_e|) / |k''_e|$, where $\delta\omega$ is the total spectral span of the pulse. For a 5 mm KDP crystal, the maximum time window is 360 fs and the bandwidth is limited to 480 mrad fs⁻¹ for the central wavelength of 830 nm.

Taking the above analysis into account, the spectral phase was reconstructed for pulses of different bandwidth and central wavelength. The plots in Fig. 2 represent the following cases: (a) pulses with the time support close to the theoretical limit—indeed, after propagation through a test block of 10 cm BK7 glass, the output pulse of the MaiTai laser is stretched to 160 fs FWHM, while the maximum time window for the 5 mm thick crystal and 10 mm thick quartz block used in the experiment is 317 fs, i.e., only twice the pulse duration FWHM; (b) pulses with central wavelength of 760 nm, close to the lower limit of the phase matching range (730 nm) and well outside the perfect GV matching region—as can be seen, accounting for the theoretical scaling factor $\alpha=0.88$, the agreement between the theory and the experiment is very good; (c) pulses of 80 mrad fs⁻¹ bandwidth, corresponding to 30 fs transform-limited pulse duration.

The effect of the pulse propagation, taking material dispersion into account, in a 20 mm nonlinear KDP crystal (with a pre-delay $t_0=1440$ fs such that the *o*- and *e*-pulses meet halfway in the crystal) on the phase reconstruction in ARAIGNEE was studied by solving numerically (using a split-step algorithm) the system of three nonlinear coupled equations for A_o , A_e , and A_{SF} . To quantify the errors in the reconstructed phase, the spectral weighted phase error was used.¹² We demonstrate the parameter range over which the input pulse can be accurately reconstructed by plotting this error for different central wavelengths and pulse bandwidths in Fig. 3. The phase error appears symmetric around the perfect phase-matching wavelength of 830 nm and for a

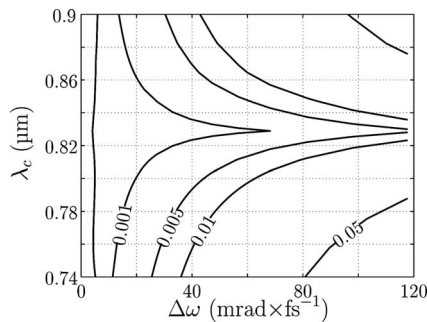


Fig. 3. Spectral phase error ϵ_ϕ of the retrieved pulse calculated from a numerical simulation of the pulse propagation in the nonlinear crystal plotted as a function of the input pulse bandwidth (intensity FWHM) and central wavelength. Gaussian transform-limited input pulse is used.

transform-limited pulse remains below 0.01 (a very conservative accuracy limit) up to a bandwidth of 120 mrad fs⁻¹ (20 fs). The error does not exceed ~ 0.01 up to 40 mrad fs⁻¹ bandwidth for the central wavelength between 740–900 nm, indicating accurate pulse reconstruction over this broad spectral range. The calculated spectral intensity error $[\sum_\omega |I_{\text{Input}}(\omega) - I_{\text{Spider}}(\omega)|^2]^{1/2}$, where the intensities are normalized to unity, is effectively negligible, being below 0.2% over the entire parameter space shown in Fig. 3. The experimental spectral phase errors for plots (a)–(c) of Fig. 2 are, respectively, 0.022, 0.005, and 0.017, while the theoretical values predicted by a numerical simulation of SF generation in a 5 mm KDP crystal are 0.024, 0.0034, and 0.0069. The comparison between the measured and numerically predicted ϵ_ϕ values shows their agreement, with the experimental values exceeding the theoretical case values. We note that the errors are minimal in the absolute sense. When matched with the results of Fig. 2, these ϵ_ϕ values provide a qualitative understanding of our ARAIGNEE performance metric.

In conclusion, a simple and robust implementation of spectral shearing interferometry with a single nonlinear crystal—ARAIGNEE—was demonstrated. We presented a detailed analytical and numerical analysis of the pulsed fields interaction in type II SFG and used it to explore the performance of the instrument, including reconstruction of the ultrashort pulses with spectral bandwidths and central frequencies at the limits of the theoretically accessible parameter ranges.

This work was supported by the Engineering and Physical Sciences Research Council, grant EP/D503248/1. A. Radunsky acknowledges the support of the National Science Foundation, and S.-P. Gorza acknowledges the support of the Wiener-Anspach Foundation. A Radunsky's e-mail address is alexr@optics.rochester.edu.

References

1. P. O'Shea, M. Kimmel, X. Gu, and R. Trebino, *Opt. Lett.* **26**, 932 (2001).
2. D. T. Reid and I. G. Cormack, *Opt. Lett.* **27**, 658 (2002).
3. C. Dorrer and I. Kang, *Opt. Lett.* **28**, 477 (2003).
4. I. Z. Kozma, P. Baum, U. Schmidhammer, S. Lochbrunner, and E. Riedle, *Rev. Sci. Instrum.* **75**, 2323 (2004).
5. C. Iaconis and I. A. Walmsley, *IEEE J. Quantum Electron.* **35**, 501 (1999).
6. A. S. Radunsky, E. M. Kosik, I. A. Walmsley, P. Wasylczyk, W. Wasilewski, A. B. U'Ren, and M. E. Anderson, *Opt. Lett.* **31**, 1008 (2006).
7. W. P. Grice, A. B. U'Ren, and I. A. Walmsley, *Phys. Rev. A* **64**, 063815 (2001).
8. A. P. Baronavski, H. D. Ladouceur, and J. K. Shaw, *IEEE J. Quantum Electron.* **29**, 580 (1993).
9. C. Dorrer, *Opt. Lett.* **24**, 1532 (1999).
10. The details of the derivation will be reported in a future publication.
11. H. Wang and A. M. Weiner, *IEEE J. Quantum Electron.* **40**, 937 (2004).
12. M. E. Anderson, L. E. E. de Araujo, E. M. Kosik, and I. A. Walmsley, *Appl. Phys. B* **70**, S85 (2000).